Structurally Distinct Modes of Recognition of the KIX Domain of CBP by Jun and CREB†

Kathleen M. Campbell‡ and Kevin J. Lumb*,‡,§

Department of Biochemistry and Molecular Biology and Department of Chemistry, Colorado State University, Fort Collins, Colorado 80523-1870

Received May 30, 2002; Revised Manuscript Received September 7, 2002

ABSTRACT: Gene expression is coordinated in part by interactions between transcriptional activators and other transcription factors such as coactivators. The KIX domain of the coactivator and histone acetyltransferase CREB binding protein (CBP) binds numerous mammalian and viral transcriptional activators such as BRCA1, CREB, c-Jun, c-Myb, p53, papillomavirus E2, and HTLV-1 Tax. Formation of the CREB−CBP complex depends on phosphorylation of the KID region of CREB and involves induced folding of KID upon binding a hydrophobic groove of the KIX domain of CBP. Here we investigate the formation of the complex formed by human KIX and the N-terminal activation domain of human c-Jun. The c-Jun activation domain and KID do not share significant sequence similarity. Circular dichroism spectroscopy shows that the Jun N-terminal activation domain is intrinsically disordered in isolation and that KIX binding is independent of Jun phosphorylation. In contrast to the mode of binding exhibited by CREB, NMR chemical shift mapping indicates that the c-Jun activation domain binds to a distinctly different surface of KIX than used by CREB. Moreover, NMR and sedimentation equilibrium studies show that the activation domains of c-Jun and CREB can simultaneously bind the KIX domain of CBP. The results illustrate a new mode of binding and combinatorial recruitment via the KIX domain of CBP by multiple transcriptional activators.

The expression of protein-coding genes involves the assembly of a large number of proteins such as RNA polymerase II, general transcription factors, activators, coactivators, and architectural proteins (*1*, *2*). Specificity for a given gene is directed in part by transcriptional activators that bind regulatory DNA sequences (*1*). Transcriptional activators contain a functionally independent DNA-binding domain and one or more activation domains that bind and localize other components of the transcription machinery to the target gene (*1*). Coactivators are important binding partners for activation domains and contribute to transcription by acting as bridging molecules between transcription factors or as enzymes that introduce regulatory modifications such as histone acetylation (*1*, *2*).

The coactivator CBP[1] is a large (265 kDa) multidomain protein containing a histone acetyltransferase domain and several protein-interacting domains that bind RNA polymerase II, the general transcription factors TFIIB and TFIID, and a legion of mammalian and viral transcriptional activators (*3*, *4*). One region of CBP that binds transcriptional activators is the autonomously folded, helical KIX domain (*5*, *6*). KIX binds inducibly to CREB upon CREB phosphorylation (*5*, *7*, *8*). KIX also binds constitutively to a range of human activators such as BRCA1, c-Jun, c-Myb, p53, and SREBP and to viral activators such as papillomavirus E2 and HTLV-1 Tax (*9*−*17*). The wide range of activator complexes involving CBP mirrors the diverse roles for CBP in processes such as cell growth, transformation, and development (*3*, *4*).

Of the numerous protein−protein complexes involving KIX, the interaction between CBP and the KID region of CREB is the most understood in molecular terms. The KIX-binding domain of CREB is called KID, which contains a phosphoryation site at Ser 118 in human CREB (Ser 133 in mouse CREB).[2] The unbound KID region is largely unfolded in both the unphosphorylated and phosphorylated forms (*5*, *6*, *18*, *19*). Upon binding KIX, phosphorylated KID adopts an ordered structure of two helices linked by a turn and binds to a shallow hydrophobic groove on one surface of KIX (*6*). Phosphorylation plays a critical role in stabilizing the pKID−KIX complex (*5*, *6*, *20*, *21*). Other activation domains have been proposed to recognize the same hydrophobic groove

† Supported by American Cancer Society Grant RSG-02-051-GMC and by NIH Equipment Grants RR11847 and RR11981. K.M.C. was supported in part by a Colorado Institute for Research in Biotechnology fellowship.

* Corresponding author. E-mail: lumb@lamar.colostate.edu.

‡ Department of Biochemistry and Molecular Biology.

§ Department of Chemistry.

[1] Abbreviations: [θ], molar ellipicity; AP-1, activating protein 1; CBP, CREB binding protein; CD, circular dichroism; CREB, CRE response element binding protein; DSS, sodium 2,2-dimethyl-2-silapentane-5-sulfonate; HPLC, high-performance liquid chromatography; HSQC, heteronuclear single-quantum coherence spectroscopy; HTLV-1, human T-cell leukemia virus 1; K_d, dissociation constant; KID, kinase-inducible domain; NMR, nuclear magnetic resonance; PCR, polymerase chain reaction; pSer, phosphorylated serine; SREBP, sterol regulatory element binding protein; TFA, trifluoroacetic acid.

[2] The KID regions of human and mouse CREB are identical across residues 85−145 of human CREB and residues 101−160 of both rat and mouse CREB. The Ser phosphorylation site of KID that moderates interactions with CBP is Ser 118 of human CREB and Ser 133 of rat and mouse CREB.

10.1021/bi026222m CCC: $22.00
Published on Web 10/30/2002

```
c-Jun       1   MTAKMETTFY  DDALNASFLP  SESGPYGYSN  PKILKQSMTL NLADPVGSLK 50
                            |     ||      |   | |
CREB        86              QISTIAE  SED-----SQ  ESVDSVTDSQ KRREILSRRP 117

c-Jun       51  PHLRAKNSDL  LTSPDVGLLK  LASPELERLI  IQSSNGHIT 89
                      |       | | |       | |
CREB        118 SYRKILNDLS  SDAPGVPRIE  EEKSEEET 145
```

FIGURE 1: Aligned sequences of the human c-Jun N-terminal activation domain (residues 1−89) and the KID region of human CREB (residues 86−145). The sequence similarity between the two full-length activation domains is insignificant, even with the inclusion of a gap in CREB to improve sequence similarity. Residues assigned as similar or identical in the sequence alignment are connected with vertical bars. Residues of c-Jun and CREB that are underlined correspond to pKID and pJun(47−89), respectively. The Ser 118 phosphorylation site of CREB is shown in bold (equivalent to Ser 133 of mouse CREB). The KID domains of mouse and human CREB are identical over the region shown.

of KIX that is occupied by the KID domain of CREB (*6*, *15*).

The human transcriptional activator c-Jun is involved in a diverse array of protein−protein interactions and cellular process such as differentiation and apoptosis as a component of AP-1 (*22*−*24*). CBP and full-length c-Jun interact to stimulate transcription in vivo (*9*). Independent studies show that the N-terminal activation domain of c-Jun binds CBP (*9*) and that KIX binds full-length c-Jun (*15*). Taken together, these studies suggest that the c-Jun−CBP interaction is mediated by the N-terminal domain of c-Jun and the KIX domain of CBP. Phosphorylated c-Jun binds CBP (*25*), although c-Jun phosphorylation is not required for the formation of the c-Jun−CBP complex (*9*, *15*).

Here we present a structural study of the c-Jun−KIX complex. Deletion studies refine the region of c-Jun that binds KIX. Strikingly, the c-Jun activation domain binds at a different surface of KIX than KID, and the KID and c-Jun activation domains can simultaneously bind KIX. Our results illustrate a novel mode of KIX binding that is different to the mechanism employed by CREB and provide new insight into the molecular basis of combinatorial recruitment of CBP by multiple activation domains.

EXPERIMENTAL PROCEDURES

Protein Production and Purification. JunAD corresponds to residues 1−89 of human c-Jun with an additional N-terminal Gly-Ser-His derived from the expression vector (Figure 1). JunAD was expressed as a His-tag fusion protein in *Escherichia coli* strain BL21(DE3) using a pET15b vector harboring a PCR product encoding residues 1−89 of human c-Jun (called pET15b-JunAD) amplified from a plasmid encoding full-length c-Jun (gift of M. Karin). The coding sequence of pET15b-JunAD was confirmed with dRhodamine automated sequencing. Cells were grown at 37 °C to an optical density at 600 nm of 0.6, induced with 0.5 mM IPTG for 3 h, harvested by centrifugation, and lysed by sonication. His-tagged JunAD was purified from the soluble cell lysate fraction with His-bind resin (Novagen), and the His tag was cleaved with thrombin (Novagen). Overdigestion with thrombin of JunAD produced Jun(1−57), identified with mass spectrometry, which corresponds to residues 1−57 of human c-Jun with an additional N-terminal Gly-Ser-His. Final purification of both proteins was by C_{18} HPLC using linear water/acetonitrile gradients containing 0.1% TFA.

Jun(47−89) is a synthetic peptide corresponding to residues 47−89 of human c-Jun with an acetylated N-terminus and amidated C-terminus (Figure 1). The peptide was synthesized with manual in situ neutralization Boc chemistry using MBHA resin (*26*). Final purification was by C_{18} HPLC using linear water/acetonitrile gradients containing 0.1% TFA.

pJun(47−89) is equivalent to Jun(47−89) except Ser 63 and Ser 73 are phosphorylated. The peptide was synthesized with manual Fmoc chemistry using Rink Amide resin. Essentially the same protocol for manual in situ neutralization Boc synthesis was used (*26*), except Fmoc groups were removed using 20% (v/v) piperidine in DMF and the peptide was cleaved with TFA. Final purification was by C_{18} HPLC using linear water/acetonitrile gradients containing 0.1% TFA.

KIX (residues 588−679 of human CBP with an additional N-terminal Met) was expressed in *E. coli* strain BL21(DE3) pLysS using the plasmid pETKIX (*20*).[3] Cells were grown to an optical density at 600 nm of 1, induced with 1 mM IPTG for 3 h, harvested by centrifugation, and lysed by sonication. The soluble cell lysate fraction was passed over HiTrap Q (Pharmacia) equilibrated in buffer A (10 mM Tris-HCl, 1 mM EDTA, and 1 mM PMSF, pH 7.5), and the flow-through was loaded onto HiTrap SP (Pharmacia) equilibrated in buffer A. KIX was eluted from the SP column with a NaCl gradient. ^{15}N-Labeled and ^{15}N/^{13}C-labeled KIX were prepared in the same way as unlabeled KIX, except cells were grown in M9 minimal medium containing $[^{15}NH_4]_2SO_4$ and/or [^{13}C]glucose as the sole nitrogen and carbon sources. Final purification of KIX was by C_{18} HPLC using linear water/acetonitrile gradients containing 0.1% TFA.

pKID (residues 100−133 of human CREB phosphorylated at Ser 118; Figure 1)[2] was synthesized with Fmoc chemistry by the Macromolecular Resources Facility at Colorado State University and purified with C_{18} HPLC using linear water/acetonitrile gradients containing 0.1% TFA as described previously (*20*).

The identity of all proteins was confirmed with electrospray mass spectrometry. In all cases the expected and observed masses agreed to within 1 Da.

Concentration Determinations. Protein concentrations were determined by absorbance spectroscopy in 6 M GuHCl and 10 mM sodium phosphate, pH 6.5 at 25 °C, using extinction coefficients at 276 nm of 12650, 4350, and 4350 M^{-1} cm^{-1} for KIX, JunAD, and Jun(1−57), respectively, and 1450 M^{-1} cm^{-1} for Jun(47−89) and pJun(47−89) (*27*).

CD Spectroscopy. CD spectra were acquired with a Jasco J720 spectrometer. Spectra were collected at 10 °C on samples containing 20 μM of each protein in 10 mM sodium phosphate and 150 mM NaCl, pH 7.0. The molar ellipicity $[\theta]$ was obtained by normalization of the measured ellipicity θ using $[\theta] = \theta \times 100/(nlc)$, where n is the total number of residues of the protein or mix of proteins, c is the total protein

[3] The KIX regions of human and mouse CBP are identical over the KIX domain used for the NMR structure determination. Residues 587−679 of human CBP are identical to residues 586−678 of mouse CBP with the exception that Thr 672 in human CBP is substituted with Ser 671 in mouse CBP. Although the human KIX domain was studied here, the mouse residue numbers are used for ease of comparison with the vast majority of studies that use the mouse sequence, including previous NMR studies of KIX complexes (*6*, *32*).

concentration in millimolar, and l is the cell path length in centimeters.

Analytical Ultracentrifugation. Sedimentation equilibrium was performed with a Beckman XL-I analytical ultracentrifuge. Data were collected in six-sector cells at rotor speeds of 30 and 40 krpm using absorbance optics for KIX and pJun(47−89) and in two-sector cells at rotor speeds of 15 and 20 krpm using interference optics for the pJun(47−89)−KIX and pJun(47−89)−pKID−KIX complexes. Samples were dialyzed against the reference buffer (10 mM sodium phosphate, and 150 mM NaCl, pH 7). Sample concentrations are given in Table 1. Masses reported in Table 1 were obtained from single species fits of the individual data sets with ORIGIN (Beckman Instruments). Masses in the text are reported as the mean mass ± standard error of the values in Table 1. Partial molar volumes were calculated as described elsewhere (*28*).

^{31}P NMR Spectroscopy. ^{31}P spectra were collected with a Varian Unity Inova operating at 202.65 MHz for ^{31}P and referenced to internal trimethyl phosphate at zero ppm.

The K_d for the pJun(47−89)−KIX complex was determined at 10 °C as 150 μM pJun(47−89) was titrated with 0−400 μM KIX. Samples were prepared in 10 mM sodium phosphate and 150 mM NaCl, pH 7.0. The K_d was obtained from changes in the ^{31}P chemical shift with KIX concentration using

$$\delta = \delta_f + \delta_b - \delta_f(P + L + K_d) - [(P + L + K_d)^2 - 4PL]^{0.5}/2[P]$$

where δ is the chemical shift at KIX concentration L, δ_f and δ_b are the free and bound chemical shifts, respectively, and P is the concentration of pJun(47−89). The fit assumes a 1:1 stoichiomtery, which was confirmed with sedimentation equilibrium.

^{31}P NMR studies of binary and ternary complex formation were performed at 10 °C on samples containing 225 μM of each protein in 10 mM sodium phosphate and 150 mM NaCl, pH 7.0. Protein concentrations were determined with absorbance spectroscopy as described above.

Chemical Shift Perturbation Mapping. Changes in KIX chemical shifts induced upon binding pKID and pJun(47−89) were measured from gradient sensitivity-enhanced ^{1}H−^{15}N HSQC spectra (*29*). Spectra were collected with a Varian Unity Inova operating at 500.13 MHz for ^{1}H and referenced to internal DSS at zero ppm. Spectra consisted of 256 complex increments defined by 112 transients and 1024 complex points. Data were processed with NMRPipe and analyzed with NMRView (*30*, *31*). Samples contained 225 μM [^{15}N]KIX, 225 μM [^{15}N]KIX and 550 μM pJun(57−89), 225 μM [^{15}N]KIX and 550 μM pKID, or 225 μM [^{15}N]-KIX, 550 μM pKID, and 550 μM pJun(57−89) in 10 mM sodium phosphate and 150 mM NaCl, pH 7.0. Changes in chemical shift are reported as $\Delta\delta = [(\Delta H^N)^2 + (\Delta N/5)^2]^{0.5}$, where ΔH^N and ΔN are the changes in amide H^N and ^{15}N chemical shifts, respectively (*32*).

Assignments for the resonances of unbound KIX at pH 5.5 and 10 °C were obtained from gradient sensitivity-enhanced HNCA and HN(CO)CA spectra (*33*−*35*). The sample comprised 600 μM [^{15}N,^{13}C]KIX in 10 mM sodium phosphate and 150 mM NaCl, pH 5.5. Assignments for KIX at 10 °C and pH 7.0 were obtained by following resonances in ^{1}H−^{15}N HSQC spectra (*29*) of 600 μM [^{15}N]KIX in 10 mM sodium phosphate and 150 mM NaCl as the pH was changed from 5.5 to 7.0 at 10 °C. Assignments for KIX in the pKID−KIX complex were obtained from the ^{1}H−^{15}N HSQC spectrum (*29*) of 225 μM [^{15}N]KIX and 550 μM pKID in 10 mM sodium phosphate and 150 mM NaCl, pH 7.0, by transferring assignments of a related phosphorylated KID−KIX complex (*32*). Assignments of KIX resonances in the pJun(47−89)−KIX complex were obtained using gradient sensitivity-enhanced HNCA and HN(CO)CA spectra (*33*−*35*) of 600 μM [^{15}N,^{13}C]KIX and 1 mM unlabeled pJun-(47−89) in 10 mM sodium phosphate and 150 mM NaCl, pH 7.0.

RESULTS

Intrinsic Disorder of the Jun Activation Domain. JunAD corresponds to the N-terminal activation domain of human c-Jun (residues 1−89; Figure 1). The CD spectrum of JunAD is reminiscent of an unfolded protein, with a minimum at 199 nm and a lack of spectral features that are characteristic of helix or sheet formation (Figure 2A). The H^N chemical shifts obtained from the HSQC spectrum of JunAD at 10 °C and pH 7.0 span 7.7−8.5 ppm (data not shown), as expected of an unfolded protein (*36*). These results indicate that the full-length N-terminal activation domain of c-Jun is intrinsically disordered or largely unfolded at neutral pH, a property shared with phosphorylated KID (*5*, *18*, *19*).

Constitutive Binding of the Jun Activation Domain and KIX. CD spectroscopy shows that unphosphorylated JunAD binds to KIX (residues 586−679 of human CBP). The CD spectrum of free KIX is indicative of a helical protein (Figure 2A), in accord with the NMR structure of the KIX domain (*6*). The CD spectrum that is expected if KIX and JunAD do not interact can be calculated from the individual spectra of the two proteins. The calculated spectrum has a smaller normalized helical signature spectrum than that of KIX alone, since the calculation reflects the contribution of the unfolded residues of unbound JunAD. Mixing of JunAD and KIX results in an increase in helicity at 222 nm over the spectrum that would be expected if the two proteins do not interact (Figure 2A).

Analytical ultracentrifugation also indicates that KIX and JunAD associate and form a 1:1 complex (Table 1). An equimolar solution of KIX and JunAD exhibits a mass of 15.5 kDa, which is within 4% of the mass expected for a 1:1 complex (Table 1). The slightly low observed mass compared to the expected mass may reflect experimental error, peptides that are not 100% active (yet must be over 90% active to give the observed mass), or incomplete formation of the complex, since 99% complex formation requires that the free ligand concentration be in 100-fold excess over the K_d (*37*).

Sedimentation equilibrium suggests that JunAD is largely monomeric, with the observed mass about 20% larger than expected for a monomer (Table 1), and that KIX is monomeric (observed mass of KIX, 11.6 ± 0.4 kDa; mass expected of a monomer, 11.1 kDa). Thus, the observed mass of the equimolar solution of KIX and JunAD is not the result of self-association of KIX or JunAD as opposed to formation of the JunAD−KIX complex.

Jun(1−57) corresponds to residues 1−57 of c-Jun (Figure 1). The CD spectrum of Jun(1−57) is reminiscent of an

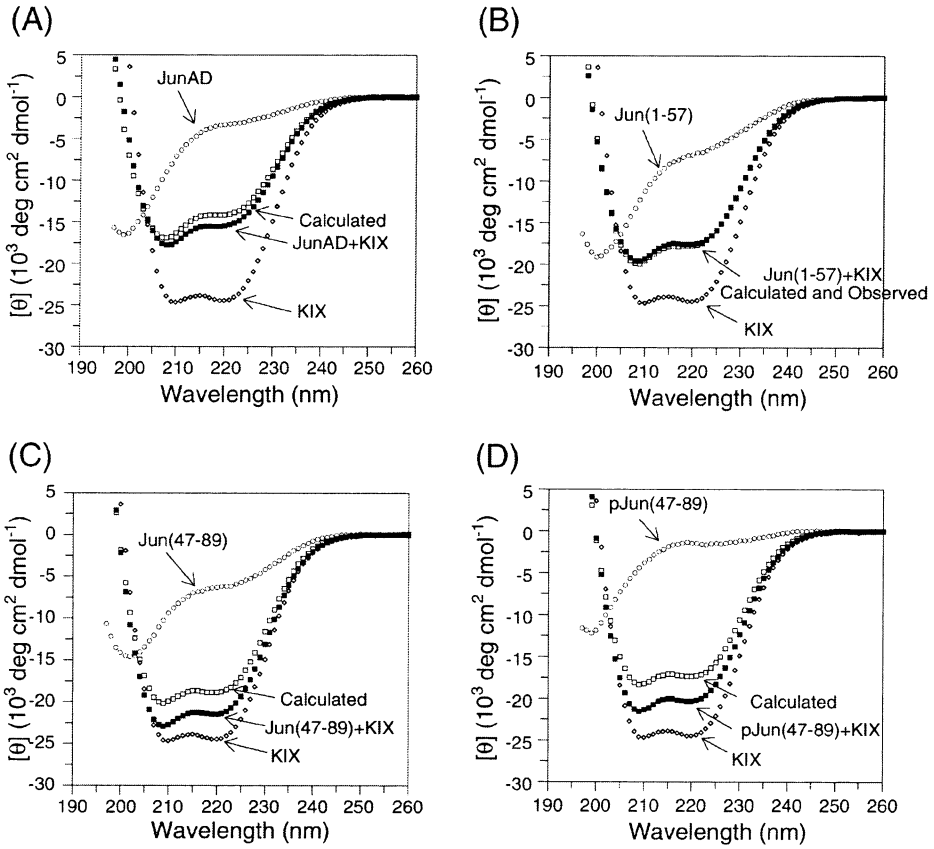

FIGURE 2: KIX forms complexes with JunAD, Jun(47−89), and pJun(47−89) but not with Jun(1−57). (A) Mixing of KIX with JunAD results in a CD spectrum with greater negative helicity at 208 and 222 nm than expected from the sum of the spectra of the two isolated proteins, suggesting that KIX binds JunAD. (B) Mixing of Jun(1−57) and KIX results in a CD spectrum that is the sum of the spectra of the two isolated proteins, suggesting that Jun(1−57) and KIX do not interact. Mixing of KIX with (C) Jun(47−89) and (D) pJun(47−89) results in CD spectra with greater helicity at 208 and 222 nm than expected from the sum of the spectra of the two isolated proteins, suggesting that KIX forms complexes with Jun(47−89) and pJun(47−89).

unfolded protein (Figure 2B), as expected since the full-length domain is unfolded (Figure 2A). Addition of Jun(1−57) to KIX results in a CD spectrum that is identical to the calculated average spectra of Jun(1−57) and KIX, suggesting that Jun(1−57) does not bind KIX (Figure 2B).

Jun(47−89) corresponds to residues 47−89 of human c-Jun (Figure 1). The CD spectrum of Jun(47−89) is characteristic of a largely unfolded protein, as expected since the full-length domain is unfolded (Figure 2A). Addition of KIX results in an observed spectrum of significantly higher helix content than expected if Jun(47−89) and KIX do not interact (Figure 2C). Essentially identical changes in the CD spectrum are observed for KIX and pJun(47−89), corresponding to Jun(47−89) with Ser 63 and Ser 73 phosphorylated (Figure 2D).

Jun(47−89) and pJun(47−89) induce greater changes than JunAD in the normalized molar ellipicity at the helical signature wavelengths of 208 and 222 nm. This presumably reflects the per residue normalization of the CD signal. The same number of residues participating in helix formation in an otherwise unfolded peptide will give a larger normalized molar ellipicity at the helical signature wavelengths of 208 and 222 nm in a shorter peptide [i.e., Jun(47−89) or pJun(47−89)] than in a longer peptide (i.e., JunAD).

The small spectroscopic changes seen upon formation of the various KIX complexes with either CD (Figure 2) or fluorescence spectroscopy (data not shown) preclude reliable K_d measurements. pJun(47−89) contains two phosphate groups that can be monitored with ^{31}P NMR spectroscopy. Changes in ^{31}P chemical shift of one of the ^{31}P resonances upon titration with KIX yield a K_d for the pJun(47−89)−KIX complex of approximately 3×10^{-5} M (Figure 3). The other resonance shifted by only 0.02 ppm, and so changes in chemical shift of this resonance were not fit to obtain a K_d [spectra of the free and bound forms of pJun(47−89) are shown in Figure 6]. The ^{31}P chemical shifts of pJun(47−89) are in fast exchange between the free and KIX-bound forms. The changes in the ^{31}P chemical shift upon titration with KIX are hyperbolic, as expected for a specific binding event (Figure 3).

The results collectively show that the unphosphorylated Jun N-terminal activation domain binds constitutively to KIX, in accord with previous molecular biology studies of full-length Jun (*15*). In addition, the results show that complex formation is essentially unaffected by c-Jun phosphorylation at Ser 63 and Ser 73, and the region of c-Jun that contacts KIX is localized to residues 47−89.

Chemical Shift Perturbation Mapping of the Jun-Binding Surface of KIX. The Jun and pKID binding sites on KIX were mapped with NMR chemical shift perturbation mapping (*38*) from the changes in ^{15}N-labeled KIX chemical shifts upon binding unlabeled pKID or pJun(47−89). Resonances from the unlabeled activation domains are not seen in ^{1}H−

Table 1: Sedimentation Equilibrium Analysis of Complex Formation[a]

total concentration (μM)	observed mass (kDa) 30 krpm	40 krpm
KIX (Expected Mass for Monomer: 11139.8 Da)		
25	11.8 (1.04)	11.4 (1.03)
38	11.3 (1.02)	11.6 (1.05)
63	11.5 (1.04)	12.2 (1.10)
pJun(47−89) (Expected Mass for Monomer: 4984 Da)		
220	5.93 (1.19)	5.49 (1.10)
330	5.84 (1.17)	5.88 (1.18)
550	5.93 (1.19)	5.84 (1.17)

total concentration (μM)	observed mass (kDa) 15 krpm	20 krpm
pJun(47−89) + KIX (Expected Mass for 1:1 Complex: 16124 Da)		
200	14.2 (0.88)	14.8 (0.92)
300	15.9 (0.99)	16.5 (1.02)
450	16.1 (1.0)	15.7 (0.97)
pJun(47−89) + pKID + KIX (Expected Mass for 1:1:1 Complex: 20104 Da)		
250	17.3 (0.86)	17.8 (0.89)
375	19.2 (0.96)	19.1 (0.95)
500	18.6 (0.95)	19.0 (0.95)

[a] Data for KIX alone, pJun(47−89) alone, equimolar pJun(47−89) + KIX, and equimolar pJun(47−89) + pKID + KIX were collected at two rotor speeds and three concentrations. The ratio of observed to expected mass is in parentheses after the observed mass.

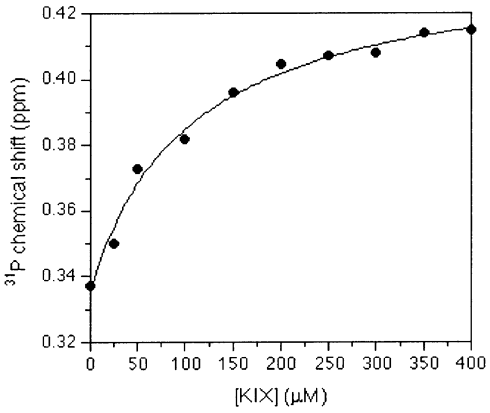

FIGURE 3: Association of KIX and pJun(47−89) monitored from the change in ^{31}P chemical shifts of pJun(47−89) with total KIX concentration. Data were fit for 1:1 complex formation to give a K_d of 3×10^{-5} M.

^{15}N HSQC spectra of the complexes. Studies at neutral pH were possible using gradient sensitivity-enhanced HSQC spectra collected with minimal water excitation (*29*).

The cross-peak resolution and sensitivity of the KIX HSQC and triple resonance spectra were significantly higher at pH 5.5 than pH 7, and so KIX was assigned at pH 5.5 using triple resonance methods. The ^{15}N and H^N chemical shifts at pH 7 and 10 °C were then obtained from changes in chemical shift with pH in HSQC spectra.

The NMR structure of the phosphorylated KID−KIX complex (*6*) was determined at pH 5.5 using different peptide fragments of CREB and CBP than used here. The NMR structure determination used a phosphorylated KID peptide corresponding to residues 101−160 of human CREB, whereas the pKID used here corresponds to residues 86−145 of human CREB phosphorylated at Ser 118 (Figure 1).

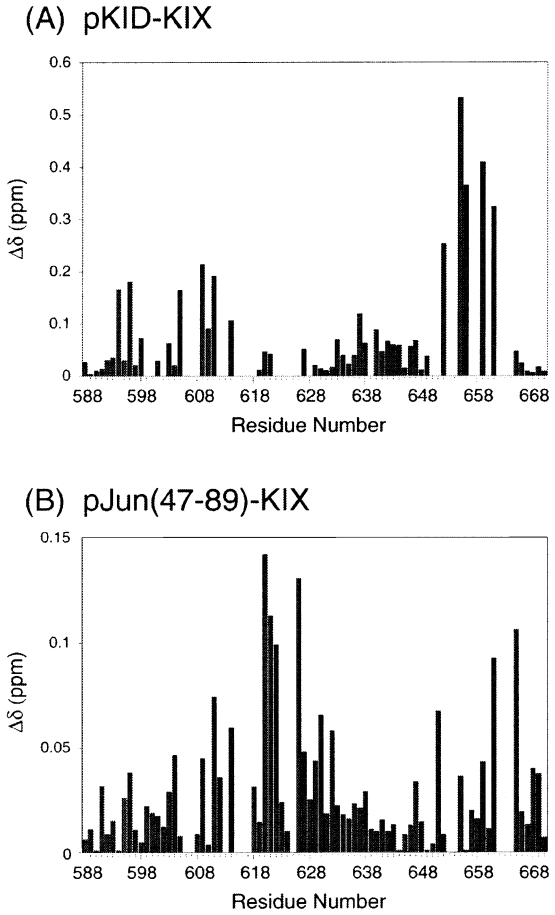

FIGURE 4: Chemical shift changes ($\Delta\delta$) induced in KIX by (A) pKID and (B) pJun(47−89). Changes are normalized averages of the amide H^N and N chemical shift changes (*32*). KIX residues that experienced a significant H^N chemical shift perturbation upon binding pJun(47−89) also had a significant N chemical shift perturbation, with the single exception of Asp 622 (for which $\Delta H^N = 0.10$ ppm and $\Delta N = 0.07$ ppm).[3]

pKID spans the folded region of CREB (*6*) and is sufficient for binding KIX (*20*). The KIX domain used here is a longer version of higher solubility (residues 588−679 of human CBP) (*20*) than used for the structure determination (residues 587−667 of human CBP) (*6*). To confirm that the KIX and pKID proteins used here at pH 7.0 bind in the same way as seen in the NMR structure of the phosphorylated KID−KIX complex determined at pH 5.5, changes in the [^{15}N]KIX chemical shifts were measured upon binding unlabeled pKID at 10 °C and pH 7.0.

Unambiguous assignments for 56 of 93 residues of KIX in the pKID−KIX complex at pH 7.0 were obtained by transferring assignments of the phosphorylated KID−KIX complex reported at pH 5.5 (*32*). The average change in KIX chemical shifts upon binding pKID is 0.08 ppm, with the largest changes (>0.2 ppm) observed for Glu 655, Lys 656, Lys 659, and Gln 661 (Figure 4).[3] Not all residues could be assigned at pH 7.0 due to chemical shift degeneracy and/or line broadening effects. However, sufficient chemical shift changes could be measured to confirm that the changes in human KIX chemical shifts upon binding human pKID agree qualitatively with those reported previously for the phosphorylated KID−KIX complex under different conditions (*32*). The KIX residues that experienced significant changes in chemical shift upon binding pKID are localized to the

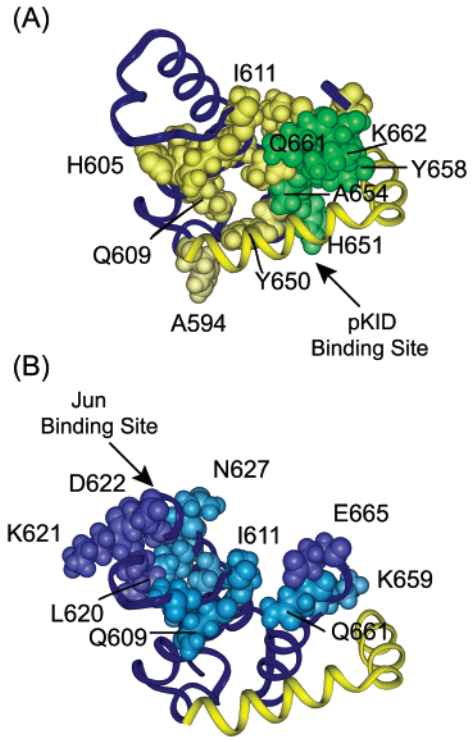

FIGURE 5: Chemical shift perturbation mapping of KIX binding sites.[3] Both pKID and pJun(47−89) cause chemical shift changes on contiguous surfaces of KIX. However, the surfaces are different, indicating that the two activation domains recognize different regions of KIX. (A) Regions of the largest chemical shift changes of KIX induced by pKID. Amino acids with chemical shift changes of 0.1−0.2 and >0.2 ppm are in yellow and green, respectively. In addition to the residues that undergo chemical shift changes measured here at pH 7.0, His 651, Ala 654, Glu 655, Tyr 658, Lys 659, Ile 661, and Lys 662 are shown. These residues have significant chemical shift changes upon binding phosphorylated KID at pH 5.5 (*32*) but could not be unambiguously assigned in this study of pKID−KIX at pH 7.0 due to chemical shift degeneracy (and are not included in Figure 4). (B) Regions of the largest chemical shift changes of KIX induced by pJun(47−89). Amino acids with chemical shift changes of 0.05−0.1 and >0.1 ppm are in light blue and dark blue, respectively. The helical ribbons of KIX and pKID are in blue and yellow, respectively. Drawn using the Protein Databank file 1kdx (*6*).

KID binding site (Figure 5), reflecting consistency between the pKID binding site obtained here with chemical shift mapping and the structure of the complex.

Resonance assignments at neutral pH of $^{15}N/^{13}C$-labeled KIX when bound to unlabeled pJun(47−89) were obtained from HNCA and HN(CO)CA spectra, and chemical shift perturbations were obtained from HSQC spectra (Figure 4). Addition of pJun(47−89) to KIX at neutral pH caused progressive changes in the ^{1}H and ^{15}N chemical shifts of KIX. The average change in chemical shift upon formation of the fully bound pJun(47−89)−KIX complex is 0.02 ppm. The largest changes in chemical shift (>0.1 ppm) were seen for Leu 620, Lys 621, Asp 622, Glu 626, and Arg 669.[3] Smaller but significant changes (>0.05 ppm) were seen for Val 604, Gln 609, Ile 611, Phe 612, Thr 614, Asn 627, Val 629, Ala 630, Ala 632, Lys 659, Gln 661, and Arg 668. These residues form a contiguous surface on KIX containing solvent-exposed hydrophobic residues (Figure 5). Some overlap in the residues affected by pKID and pJun(47−89) was seen (Figure 5), but these may reflect long-range effects due to conformational changes in other regions of the protein (*39*) rather than overlapping binding sites. The surface is different to the region of KIX that interacts with CREB in the structure of the pKID−KIX complex (Figure 5), indicating that c-Jun and CREB bind KIX at different sites.

The chemical shift perturbations induced by pJun(47−89) are somewhat smaller than those induced by pKID (Figure 4). The largest perturbations in chemical shift are likely to arise from changes in ring current effects resulting from conformational changes of aromatic rings (*40*). In the phosphorylated KID−KIX complex, Tyr 640, Tyr 649, Trp 591, and Tyr 658 of KIX, and Tyr 134 of pKID, are all within the vicinity of the KID binding site (*6*). In contrast, the only aromatic side chain of KIX in the vicinity of the Jun binding site is Tyr 631, and pJun(47−89) contains only a single, C-terminal Tyr. The H^N and ^{15}N chemical shifts of Tyr 631 of KIX do not change upon binding pJun(47−89), suggesting that Tyr 631 is relatively unperturbed upon complex formation. The larger number of aromatic rings, and associated ring current sources of conformationally dependent chemical shift (*40*), in the pKID binding site and of pKID may account for the larger chemical shift changes induced in KIX upon binding pKID.

pJun(47−89) and KID Simultaneously Bind KIX. The different KIX binding surfaces utilized by pKID and the c-Jun activation domain suggest that the CREB and c-Jun domains can bind KIX simultaneously. Analytical ultracentrifugation and ^{31}P NMR spectroscopy were used to monitor formation of KIX binary and ternary complexes.

Sedimentation equilibrium indicates that KIX, pJun(47−89), and pKID associate and form a ternary complex (Table 1). The observed mass of 18.5 ± 0.8 kDa is in accord with the value expected of the 1:1:1 ternary complex of 20.1 kDa (Table 1). If the ternary complex did not form, then the apparent mass would reflect the weight average of the populations of the various species, i.e., the masses of the pJun(47−89)−KIX and pKID−KIX binary complexes and the masses of the unbound proteins [since the three peptides are equimolar, exclusive binding of one activation domain over another would result in free pJun(47−89) and pKID]. The slightly low value of the observed compared to expected mass may reflect experimental error, peptides that are not 100% active (yet must be over 90% active to give the observed mass), or incomplete formation of the complex at the concentrations used.

Solution ^{31}P NMR experiments also provide evidence for the formation of the pKID−pJun(47−89)−KIX ternary complex (Figure 6). The Ser 118 ^{31}P resonances of unbound pKID and KIX-bound pKID are in slow exchange, such that dissociation of pKID is detected by the presence of a ^{31}P resonance at the chemical shift of free pKID. The Ser 63 and Ser 73 ^{31}P resonances of pJun(47−89) in free and KIX-bound states are in fast exchange, such that complete dissociation of pJun(47−89) would be detected as a resonance at the chemical shift of unbound pJun(47−89).

Addition of equimolar KIX to either pKID or pJun(47−89) causes changes in the chemical shifts of the ^{31}P resonances that reflect essentially complete formation of the complex (Figure 6). The resonances of an equimolar solution of KIX, pKID, and pJun(47−89) fall at the values seen for the binary pKID−KIX and pJun(47−89)−KIX complexes, suggesting that the three proteins form a ternary complex with pKID and pJun(47−89) occupying the same binding

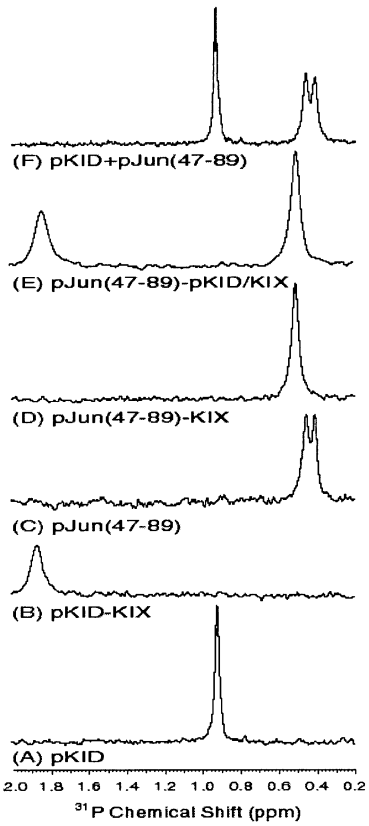

FIGURE 6: KIX can simultaneously bind pKID and pJun(47−89). ^{31}P chemical shifts of the pSer resonances were used as probes of the free and bound states of pKID and pJun(47−89). Formation of the binary KIX complexes causes changes in the ^{31}P resonances of pKID (compare spectra A and B) and pJun(47−89) (compare spectra C and D). These same changes are also induced when the three proteins are mixed together, suggesting formation of the ternary KIX−pKID−pJun(47−89) complex (spectra E). Mixing of pKID and pJun(47−89) in the absence of KIX does not result in any chemical shift changes (compare spectra A and B with spectrum F). Proteins are present in equimolar amounts with no indication of either unbound pKID or pJun(47−89) in the presence of KIX.

sites of KIX as in the bimolecular complexes. No evidence is seen for unbound pKID or pJun(47−89) in the equimolar solution. The ^{31}P chemical shifts of pKID and pJun(47−89) are not changed upon mixing the two domains in the absence of KIX, indicating that pKID and pJun(47−89) do not form a binary complex.

The combination of ^{31}P and sedimentation equilibrium results indicates that KIX, pKID, and pJun(47−89) form a ternary complex, in accord with the distinct binding sites on KIX for these two activation domains.

DISCUSSION

Formation of protein−protein complexes involving transcriptional activators and coactivators constitutes a central component to the regulation of gene expression (*1*, *2*). The KIX domain of the coactivator and histone acetyltransferase CBP binds numerous activation domains (*3*, *4*). Formation of the complex between the activator CREB and the KIX domain of CBP is inducible upon Ser 118 phosphorylation of the KID region of CREB (or Ser 133 of mouse CREB) (*5*, *8*).[2] In contrast, other activators bind constitutively to KIX without a requirement for posttranslational modification. Examples of constitutive KIX-binding activators include the mammalian activators BRCA1, c-Jun, c-Myb, p53, Sap1a, and SREBP and the viral activators papillomavirus E2 and HTLV-1 Tax (*9*−*17*).

Previous studies showed that the N-terminal activation domain of c-Jun binds CBP (*9*) and that KIX binds full-length c-Jun (*15*), suggesting that the c-Jun−CBP interaction is mediated by the N-terminal domain of c-Jun and the KIX domain of CBP. Although both the N-terminal c-Jun activation domain and the KID region of CREB domains bind KIX, the two domains do not share significant sequence similarity (Figure 1).

We show here that the Jun N-terminal domain forms a specific complex with KIX independently of Jun phosphorylation. The combination of a hyperbolic binding curve, discrete mass expected for a 1:1 complex, and localized binding surface of KIX collectively shows that KIX and the Jun N-terminal activation domain associate to form a binary complex. The first 57 residues of Jun are not sufficient to bind KIX, and the KIX-binding domain is localized to residues 47−89 of c-Jun. The K_d for formation of the KIX−pJun(47−89) complex at approximately 30 μM is comparable to the K_d of 9.7 μM for the pKID−KIX complex (*20*).

CD and ^{1}H chemical shifts suggest that the full-length c-Jun activation domain is largely unfolded or intrinsically disordered. This property is shared with many other full-length activation domains, including the KID region of CREB (*6*, *41*, *42*). The data do not, however, preclude the presence of transiently existing folded structure within the Jun activation domain, as seen for the phosphorylated KID (*18*, *19*) and p53 activation domains (*43*) and for other intrinsically disordered proteins such as the cyclin-dependent kinase inhibitor p27^{Kip1} (*44*).

CD studies indicate that the association of KIX and c-Jun is accompanied by secondary structure (helix) formation. Since KIX is a compact, helical protein (*6*), whereas the unbound Jun activation domain is unfolded, it seems likely that the Jun domain folds into a helical structure upon binding KIX. Such behavior is seen for pKID (*6*). The extent of induced helix upon binding is small, as seen with other activation−domain complexes. For example, KID forms two short (10 and 12 residue) helices upon binding KIX, p53 forms a 13-residue helix upon binding MDM2, and 11 residues of VP16 become helical on binding TAF$_{II}$31 (*6*, *45*, *46*).

Strikingly, c-Jun and CREB utilize structurally distinct modes to recognize the small, globular KIX domain of CBP. NMR chemical shift perturbations are sensitive probes of protein−protein interaction surfaces (*38*). The complex relationship between chemical shift and structure precludes detailed interpretations of chemical shift changes (*38*). However, the approach is robust when a contiguous and discrete surface of a protein is affected (*38*), as seen here for both the pKID and pJun(47−89) complexes. Chemical shift perturbation mapping reveals two distinct surfaces of comparable size on KIX that accommodate CREB and c-Jun (Figure 5). The two distinct binding sites on KIX for the CREB and c-Jun activation domains allow KIX to bind the two activation domains simultaneously, as shown here with analytical ultracentrifugation and NMR spectroscopy.

KID is largely unfolded in isolation and folds to form two helices upon binding KIX (*6*). The coupled folding and

binding event introduces a significant entropy barrier to binding (*21*), which is compensated for upon KID phosphorylation by an unusually large electrostatic contribution of the phosphate group to the binding free energy (*20*, *21*). Inducible formation of the CREB−CBP complex is thus under thermodynamic control by phosphorylation. As for KID, the N-terminal activation domain of c-Jun is devoid of significant preformed helical structure, and formation of the Jun−KIX complex results in an increase in helical structure formation. Unlike KID, the results presented here and elsewhere (*9*, *15*) show that c-Jun phosphorylation is not a prerequisite for binding KIX. c-Jun phosphorylation, therefore, does not make a critical contribution to the binding enthalpy to overcome the entropy penalty associated with folding upon binding. Instead, chemical shift perturbation mapping shows that c-Jun binds to a different surface of KIX than phosphorylated KID and, in doing so, presumably forms protein−protein interactions that make a more favorable enthalpic contribution to binding than realized by phosphorylated KID.

Other transcriptional activators may employ the c-Jun-binding site of KIX. For example, HTLV-1 Tax competes with c-Jun but not with CREB for binding KIX (*15*), suggesting that Tax might bind to a surface of KIX similar to that observed here for c-Jun. In addition, Tax competes with p53 for binding the KIX domain of CBP (*14*, *47*), and with MyoD for binding the p300 KIX domain (*48*), which raises the possibility that p53 and MyoD utilize the Tax, and hence c-Jun, binding site of KIX. The MLL (mixed-lineage leukemia) gene product can also bind KIX simultaneously with CREB (*49*) and possibly binds the same site on KIX as c-Jun. Confirmation that MLL, MyoD, Tax, and p53 use the c-Jun-binding site of KIX awaits further studies of the complexes.

Multiple contacts between transcription factors contribute greatly to transcriptional synergy and assembly of the enhancesome (*1*, *50*). Upstream regulatory sequences typically contain binding sites for multiple activators. For example, the tyrosine hydroxylase gene contains both AP-1 and CREB sites (*51*). The findings presented here show that activation domains from c-Jun and CREB can bind KIX simultaneously, thereby allowing combinatorial targeting of CBP through the KIX domain at genes that contain both AP-1 and CREB sites. Different domains of CBP can be targeted by multiple transcription factors, which opens up the possibility of synergistic interactions between CBP and other transcription factors (*3*, *4*). In addition, the simultaneous binding of the KIX domain of CBP by two different transcriptional activators that target the c-Jun and CREB binding sites of KIX may contribute greatly to the specificity and synergy of gene expression by resulting in the enhanced recruitment of CBP to target promoters. This could be especially true in the case of CBP, since CBP is thought to be present in limiting quantities in the cell (*52*, *53*).

In conclusion, we have shown that c-Jun binds the KIX domain at a new and distinct site to that utilized by CREB. This finding implies that the use of different surfaces of KIX by transcription factors provides both a mechanism to discriminate between inducible and constitutive activators and a mechanism for the combinatorial recruitment of CBP by multiple activation domains.

ACKNOWLEDGMENT

We thank R. H. Goodman and M. Karin for plasmids and C. D. Rithner and A. C. Vendel for valuable discussions.

SUPPORTING INFORMATION AVAILABLE

NMR assignments of KIX at pH 5.5 and 7.0 and the pJun-(47−89)−KIX complex at pH 7.0. This material is available free of charge via the Internet at http://pubs.acs.org.

REFERENCES

1. Ptashne, M., and Gann, A. (1997) *Nature 386*, 569−577.
2. Näär, A. M., Lemon, B. D., and Tjian, R. (2001) *Annu. Rev. Biochem. 70*, 475−501.
3. Goodman, R. H., and Smolik, S. (2000) *Genes Dev. 14*, 1553−1577.
4. Chan, H. M., and La Thangue, N. B. (2001) *J. Cell Sci. 114*, 2363−2373.
5. Parker, D., Ferreri, K., Nakajima, T., LaMorte, V. J., Evans, R., Koerber, S. C., Hoeger, C., and Montminy, M. R. (1996) *Mol. Cell. Biol. 16*, 694−703.
6. Radhakrishnan, I., Pérez-Alvarado, G. C., Parker, D., Dyson, H. J., Montminy, M. R., and Wright, P. E. (1997) *Cell 91*, 741−752.
7. Chrivia, J. C., Kwok, R. P. S., Lamb, N., Hagiwara, M., Montminy, M. R., and Goodman, R. H. (1993) *Nature 365*, 855−859.
8. Kwok, R. P. S., Lundblad, J. R., Chrivia, J. C., Richards, J. P., Bachinger, H. P., Brennan, R. G., Roberts, S. G. E., Green, M. R., and Goodman, R. H. (1994) *Nature 370*, 223−226.
9. Bannister, A. J., Oehler, T. W., D., Angel, P., and Kouzarides, T. (1995) *Oncogene 11*, 2509−2514.
10. Dai, P., Akimaru, H., Tanaka, Y., Hou, D. X., Yasukawa, T., Kanei-Ishii, C., Takahashi, T., and Ishii, S. (1996) *Genes Dev. 10*, 528−540.
11. Janknecht, R., and Nordheim, A. (1996) *Oncogene 12*, 1961−1969.
12. Oelgeschläger, M., Janknecht, R., Krieg, J., Schreek, S., and Lüscher, B. (1996) *EMBO J. 15*, 2771−2780.
13. Oliner, J. D., Andresen, J. M., Hansen, S. K., Zhou, S., and Tjian, R. (1996) *Genes Dev. 10*, 2903−2911.
14. Van Orden, K., Giebler, H. A., Lemasson, I., Gonzales, M., and Nyborg, J. K. (1999) *J. Biol. Chem. 274*, 26321−26328.
15. Van Orden, K., Yan, J.-P., Ulloa, A., and Nyborg, J. K. (1999) *Oncogene 18*, 3766−3772.
16. Lee, D., Lee, B., Kim, J., Kim, D. W., and Choe, J. (2000) *J. Biol. Chem. 275*, 7045−7051.
17. Pao, G. M., Janknecht, R., Ruffner, H., Hunter, T., and Verma, I. M. (2000) *Proc. Natl. Acad. Sci. U.S.A. 97*, 1020−1025.
18. Hua, Q., Jia, W., Bullock, B. P., Habener, J. F., and Weiss, M. A. (1998) *Biochemistry 37*, 5858−5866.
19. Radhakrishnan, I., Perez-Alvarado, G. C., Dyson, H. J., and Wright, P. E. (1998) *FEBS Lett. 430*, 317−322.
20. Mestas, S. P., and Lumb, K. J. (1999) *Nat. Struct. Biol. 6*, 613−614.
21. Parker, D., Rivera, M., Zor, T., Henrion-Caude, A., Radhakrishnan, I., Kumar, A., Shapiro, L. H., Wright, P. E., Montminy, M., and Brindle, P. K. (1999) *Mol. Cell. Biol. 19*, 5601−5607.
22. Chinenov, Y., and Kerppola, T. K. (2001) *Oncogene 20*, 2438−2452.
23. Shaulian, E., and Karin, M. (2001) *Oncogene 20*, 2390−2400.
24. Vogt, P. K. (2001) *Oncogene 20*, 2365−2377.
25. Arias, J., Alberts, A. S., Brindle, P., Claret, F. X., Smeal, T., Karin, M., Feramisco, J., and Montminy, M. (1994) *Nature 370*, 226−229.
26. Schnölzer, M., Alewood, P., Jones, A., Alewood, D., and Kent, S. B. H. (1992) *Int. J. Pept. Protein Res. 40*, 180−193.
27. Edelhoch, H. (1967) *Biochemistry 6*, 1948−1954.
28. Laue, T. M., Shah, B. D., Ridgeway, T. M., and Pelletier, S. L. (1992) in *Analytical Ultracentrifugation in Biochemistry and Polymer Science* (Harding, S. E., Rowe, A. J., and Horton, J. C., Eds.) pp 90−125, The Royal Society of Chemistry, Cambridge.
29. Kay, L., Keifer, P., and Saarinen, T. (1992) *J. Am. Chem. Soc. 114*, 10663−10665.
30. Johnson, B. A., and Blevins, R. A. (1994) *J. Biomol. NMR 4*, 603−614.
31. Delaglio, F., Grzesiek, S., Vuister, G. W., Zhu, G., Pfeifer, J., and Bax, A. (1995) *J. Biomol. NMR 6*, 277−293.

32. Radhakrishnan, I., Pérez-Alvarado, G. C., Parker, D., Dyson, H. J., Montminy, M., and Wright, P. E. (1999) *J. Mol. Biol. 287*, 859−865.
33. Ikura, M., Kay, L. E., and Bax, A. (1990) *Biochemistry 29*, 4659−4667.
34. Bax, A., and Ikura, M. (1991) *J. Biomol. NMR 1*, 99−104.
35. Kay, L. E., Xu, G. Y., and Yamazaki, T. (1994) *J. Magn. Reson. A109*, 129−133.
36. Wishart, D., and Case, D. A. (2001) *Methods Enzymol. 338*, 3−34.
37. Creighton, T. E. (1993) *Proteins: Structures and Molecular Properties*, W. H. Freeman and Co., New York.
38. Zuiderweg, E. R. P. (2002) *Biochemistry 41*, 1−7.
39. Lumb, K. J., Cheetham, J. C., and Dobson, C. M. (1994) *J. Mol. Biol. 235*, 1072−1087.
40. Perkins, S. J. (1982) *Biol. Magn. Reson. 4*, 193−336.
41. Cho, H. S., Liu, C. W., Damberger, F., Pelton, J., Nelson, H., and Wemmer, D. (1996) *Protein Sci. 5*, 262−269.
42. Campbell, K. M., Terrell, A. R., Laybourn, P. J., and Lumb, K. J. (2000) *Biochemistry 39*, 2708−2713.
43. Lee, H., Mok, K. H., Muhandiram, R., Park, K., Suk, J., Kim, D., Chang, J., Sung, Y. C., Choi, K. Y., and Han, K. (2000) *J. Biol. Chem. 275*, 29426−29432.
44. Bienkiewicz, E. A., Adkins, J. N., and Lumb, K. J. (2002) *Biochemistry 41*, 752−759.
45. Kussie, P. H., Gorina, S., Marechal, V., Elenbaas, B., Moreau, J., Levine, A. J., and Pavletich, N. P. (1996) *Science 274*, 948−953.
46. Uesugi, M., Nyanguile, O., Lu, H., Levine, A. J., and Verdine, G. L. (1997) *Science 277*, 1310−1313.
47. Colgin, M. A., and Nyborg, J. K. (1998) *J. Virol. 72*, 9396−9399.
48. Riou, P., Bex, F., and Gazzolo, L. (2000) *J. Biol. Chem. 275*, 10551−10560.
49. Ernst, P., Wang, J., Huang, M., Goodman, R. H., and Korsmeyer, S. J. (2001) *Mol. Cell. Biol. 21*, 2249−2258.
50. Carey, M. (1998) *Cell 92*, 5−8.
51. Ghee, M., Baker, H., Miller, J. C., and Ziff, E. B. (1998) *Mol. Brain Res. 55*, 101−114.
52. Kamei, Y., Xu, L., Heinzel, T., Torchia, J., Kurokawa, R., Gloss, B., Lin, S. C., Heyman, R. A., Rose, D. W., Glass, C. K., and Rosenfeld, M. G. (1996) *Cell 85*, 403−414.
53. Horvai, A. E., Xu, L., Korzus, E., Brard, G., Kalafus, D., Mullen, T. M., Rose, D. W., Rosenfeld, M. G., and Glass, C. K. (1997) *Proc. Natl. Acad. Sci. U.S.A. 94*, 1074−1079.

BI026222M